

Simulation of Time Expansion Chamber Electric  
Field

Clay Lindsay

May 4, 2005

## **Abstract**

The TRIUMF Weak Interaction Symmetry Test, or TWIST, seeks to study polarized muon-to-positron decays to high precision in order to test symmetries in the weak interaction. TWIST's 2004 data run included the addition of a sub-detector to the main apparatus in order to precisely characterize the muon beam: a time expansion chamber (TEC). On first analysis of this data run, the time expansion chamber's response produced unexpected results. The response expectations assumed a constant electric field within the TEC's modules. A detailed study of the electric field within the TEC is necessary to properly understand and predict the TEC's response for future data runs. This report describes the TEC geometry, a simulation of that geometry, and a numerical solution for the electric field inside the modules. Geometry modifications are explored and recommendations are made with regard to these modifications.

# Contents

<b>1</b>	<b>Introduction</b>	<b>3</b>
<b>2</b>	<b>Discussion</b>	<b>5</b>
2.1	Description of Techniques . . . . .	5
2.1.1	Finite Element Method . . . . .	5
2.1.2	FEMLAB Package . . . . .	6
2.1.3	The TEC Simulation . . . . .	7
2.2	Simulated Electric Field . . . . .	10
2.2.1	Wall Effects . . . . .	12
2.2.2	Drift Volume Separation . . . . .	13
2.2.3	Edge Effects . . . . .	14
2.2.4	Module Interference . . . . .	15
2.3	TEC Modifications . . . . .	17
2.3.1	Grid Plane Extension . . . . .	17
2.3.2	Module Separators . . . . .	18
2.3.3	Mylar Field-cage . . . . .	19
<b>3</b>	<b>Conclusions</b>	<b>22</b>

## List of Figures

1	3D TEC module diagram . . . . .	4
2	Parallel plate model . . . . .	4
3	Simulation geometry . . . . .	7
4	Plane potential VS wires strip comparison . . . . .	8
5	Increasing plane potential resolution . . . . .	9
6	Field cage resolution comparison . . . . .	10

7	Sense/Grid plane resolution comparison . . . . .	11
8	Electric field - X component . . . . .	11
9	Electric field - Y component . . . . .	12
10	Wall Effects . . . . .	13
11	Sense Plane Effects . . . . .	14
12	Interference - X Component . . . . .	16
13	Interference - Y Component . . . . .	16
14	Interference = Z Component . . . . .	17
15	Grid Extension Geometry . . . . .	18
16	Grid Extension Effects . . . . .	19
17	Field Cage Extension Geometry . . . . .	20
18	Field Cage Extension Interference - X . . . . .	20
19	Field Cage Extension Interference - Y . . . . .	21
20	Field Cage Extension Interference - Z . . . . .	21
21	Aluminized Mylar Field Cage . . . . .	22

# 1 Introduction

A Time Projection Chamber (TPC) is a drift chamber with a large drift volume and sense wires stretching perpendicular to the drift direction. A small and precise electric field is set up within the large drift region. When a charged particle passes through the chamber it ionizes the gas, releasing electrons to drift in the direction of the field at a relatively low velocity. The time taken for the charge to be detected by the sense wires is on the order of microseconds. These long drift times allow for high spacial precision if the electric field is precise.

While the use of a small electric field, and resulting long drift time, can produce high spacial precision, efficiency of the sense wires is reduced. Lacking a large acceleration near the sense wires, the freed electrons do not produce the desired “avalanche” effect, which is the further ionization of gas near the wires due to increased velocity. Overcoming this obstacle, a Time Expansion Chamber (TEC) is a TPC with a divided drift region. A large volume of the region has a low electric field providing long drift times. A small section of the drift region, near the sense wires, has very high field, producing the desired “avalanche” effect.

Placed in front of the main TWIST spectrometer, the purpose of the TWIST’s TEC is to precisely measure beam characteristics. The TEC consists of two modules; one for measuring each coordinate (x and y). Figure 1 shows a single module.

The main drift region is defined by two planes. A solid high voltage plane at the bottom of the module at -1kV and a grounded grid plane at the top of the drift region. The separation between the two is roughly 60mm, setting up an average electric field of about 16.6 V/mm in the downward direction. The design is modeled from the resulting field of two parallel potential plates as

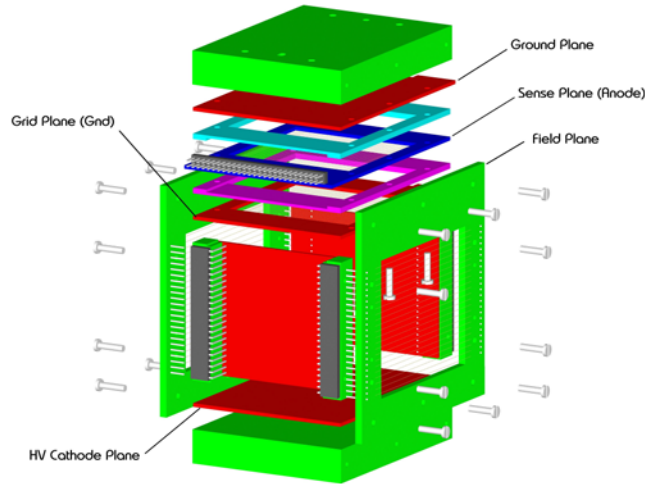


Figure 1: Blown up TEC module. Shown are the 4 main components of the module: sense plane, grid plane, field-cage and high voltage cathode plane.

seen in figure 2. While the field is constant when the plate's separation is far smaller than their length, this is not the case for the TWIST TEC modules. To compensate for the resulting edge effects of the plates, the TEC is surrounded by a field-cage, which are wires at a set potential intended to shape the field and negate the edge effects.

The “gain” drift region is defined by the ground grid plane described above

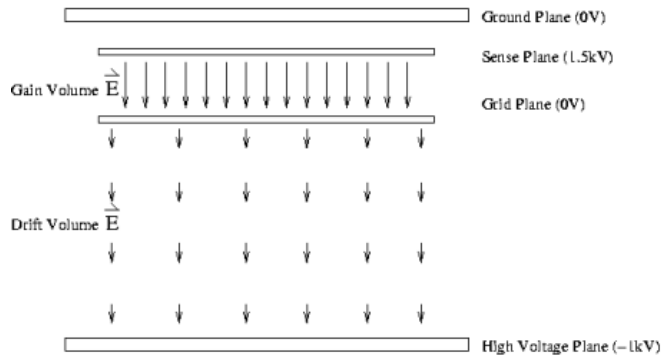


Figure 2: Parallel plate base model for TEC modules.

and the sense wires themselves. The sense wires are held at a potential of 1500kV and positioned 4mm from the grounded grid plane. The result is an average field of 375V/mm in the downward direction; sufficient for drift electrons to produce high gain through the “avalanche” effect.

The two modules are identical and are positioned in a gas chamber 40mm apart and rotated 90 degrees. This design allows for a high-gain, spatially resolute measurement of particle position in both x and y coordinates. Problems arise with this design when considering how the positioning, gas chamber and module layout affect the electric field in the drift region.

## 2 Discussion

### 2.1 Description of Techniques

#### 2.1.1 Finite Element Method

The electric field of the TEC is too complex to determine with analytic methods. While an approximate solution can be produced, such a solution is not accurate enough to examine small deviations in the field. Changes on the percentage scale compound into large spacial inaccuracies as the drift times depend on the integral of the field from the point of ionization to the sense wires. Analytic approximations to the field in the drift regions are simply not sufficient. Numerical methods must be employed.

The finite element method is a common tool used to solve partial differential equations on complex surfaces. Determining the electric field of the TEC involves solving Poisson’s equation for the known surface potentials. The method involves breaking the continuous surface into discrete elements and solving Poisson’s equation for each individual boundary condition, ensuring continuity in a solution. This effectively reduces the problem from a complex partial differen-

tial equation to a set of linear differential equations which can be solved with a simple matrix elimination method.

### **2.1.2 FEMLAB Package**

The FEMLAB package employs the finite element method to solve partial differential equations on complex surfaces. FEMLAB's electrostatics package allows for electric field calculations on defined potential surfaces and employs a solver optimized for electrostatic problems. FEMLAB provides accurate construction of geometry and quick solving methods; but, it has its limitations.

The process of breaking each surface into elements is called "meshing". FEMLAB takes each surface and randomly defines tetrahedral regions of varying size. This process is automated in FEMLAB and problems occur when there are large scale differences in geometry. In order to accurately mesh relatively small regions (eg. wire thicknesses compared to gas box length) a very large amount of small elements are necessary. A large number of small elements leads to a large number of linear differential equations to solve, and thus, a large matrix for the solver. This leads to the computational limit of FEMLAB's employment of the finite element method: memory.

Assuming a computer with the capability to address the necessary amount of memory, and assuming processing time scales linearly after physical memory is exhausted, the computation of the electric field of the geometry described above would take approximately 40 days. This is impractical for a study requiring multiple field calculations. With some approximations the FEMLAB package can be used to do a qualitative study of the TEC field on a timescale of about 4-6 hours per solution.

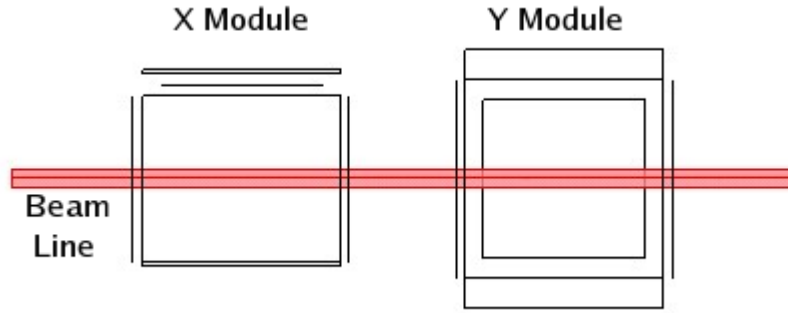


Figure 3: A capture of the simulation geometry from the FEMLAB package. Shown are the two modules with beam-line in pink down the center.

### 2.1.3 The TEC Simulation

Two main approximations were made in the FEMLAB simulation to accommodate computational limitations.

The first approximation involves the omission of non-conducting materials in the simulation. Figure 3 shows the simulation geometry. The modules are simulated as the 4 wire-planes and 4 conducting planes. The field cage planes, sense plane and grid plane are taken to be zero thickness; the wires and conducting strips are taken as rectangular strips. This approximation allows for a reduction of small scale volume elements in the modules. This is a reasonable approximation, as the thicknesses of the wires and strips are on the 10 micron scale.

The second approximation involves the use of defined potential planes to represent the wires. Use of physical wire strips in the FEMLAB simulation effectively forces small-scale meshing on each wire. This leads to a large number of small elements representing the surface. Figure 4 shows two meshings of the sense plane. The first is a mesh using physical wire strips. The second is the “plane of defined potential”. The plane potential method involves meshing a plane uniformly and explicitly defining a coordinate-dependent potential.

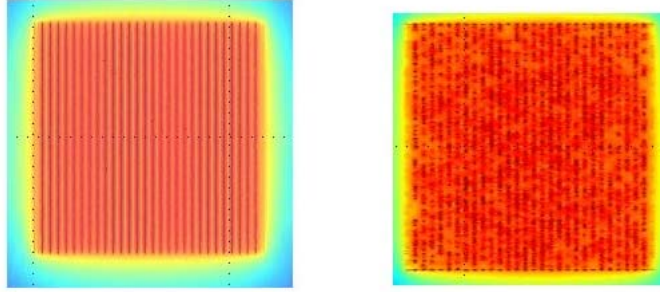


Figure 4: Sense plane represented as forced mesh wires (right) and defined plane potential (left). Roughness in plane potential is due to randomized placement of tetrahedral elements. Potential is set per element depending on element center position.

When an element is assigned to a position, it is assigned a potential at the center of its tetrahedron. By generating a uniform, but random, meshing with small elements, on average, the wire is well represented. The defined potential mesh appears “rough” because not all of the tetrahedra centers fall on the wire positions.

Figure 5 shows the effect of resolution increases in the defined potential plane. The standard resolution used for results is shown as the 8x base resolution. At this resolution the number of elements used in the meshing is  $1/6$  that of physical forced mesh wires.

The plane potential approximation allows a resolution dependent accuracy in wire meshing. This accuracy can be tested against the strip meshing in the context of the TEC geometry.

Figure 6 shows dominant field in a single module for varying field cage resolutions. The cage meshing shows a large impact in the shape of the field. Approaching the wire-planes, the 3 resolutions plots separate, due to the poor representation of the plane in the lower resolutions. Shown also is the field when physical strips are used to force meshing on the wires. The 8x resolution wire

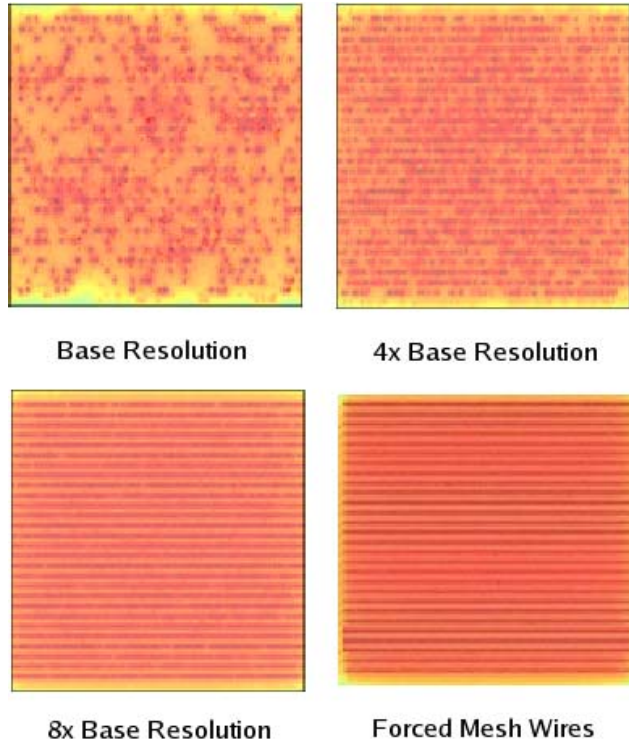


Figure 5: A comparison of sense plane potentials for increasing resolution. Standard simulations employ the 8x base resolution listed above. Shown also is the sense plane with forced wire meshing, increasing the element count by a factor of 6 from the 8x base resolution.

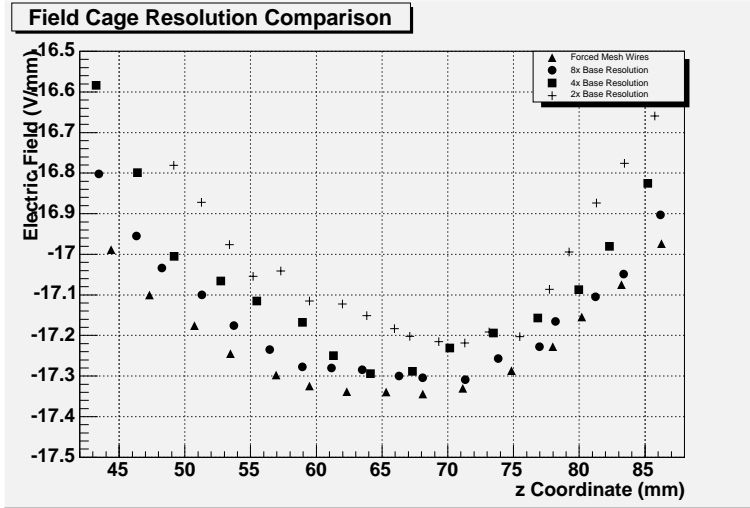


Figure 6: Dominant field on beam axis ( $Z$ ) down the center of a single module. Shown are comparisons of field cage resolutions, demonstrating the effect of field cage resolution on simulation results.

planes are a good approximation to the forced meshing strips and reduce the number of elements by approximately a factor of 6.

Figure 7 shows the dominant field in single module for varying grid/sense plane resolutions. The difference is mainly in the magnitude of the field towards the center of the module. Also shown is the forced meshing wire strips. The 8x base resolution is a good approximation to the physical strips.

## 2.2 Simulated Electric Field

Using a resolution of 8x base as discussed above, the electric field was solved for the nominal setup. Figures 8 and 9 show the  $x$  and  $y$  components of the electric field across the entire gas-box. Ideally, the field inside of the module regions should be flat. On first examination, the field varies by about 2.4 V/mm (15% of dominant field) across the length of each module.

There are 4 main areas where irregularities could arise in the electric field:

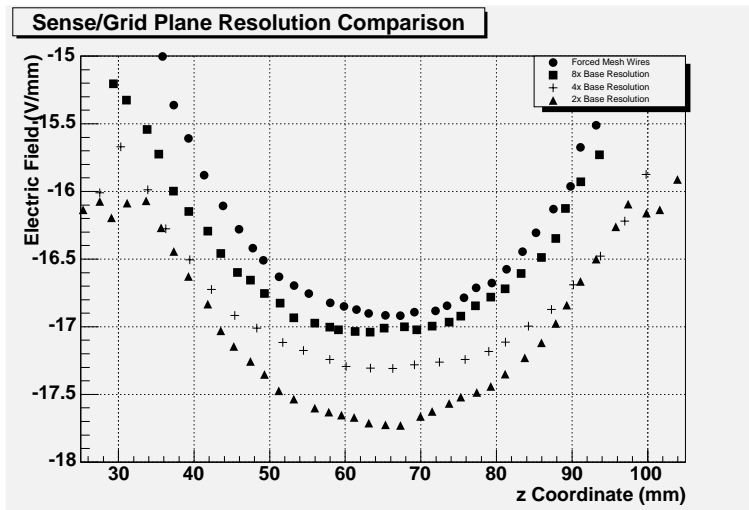


Figure 7: Dominant field on beam axis ( $Z$ ) down the center of a single module. Shown are increasing resolutions in sense and grid planes, demonstrating the effective

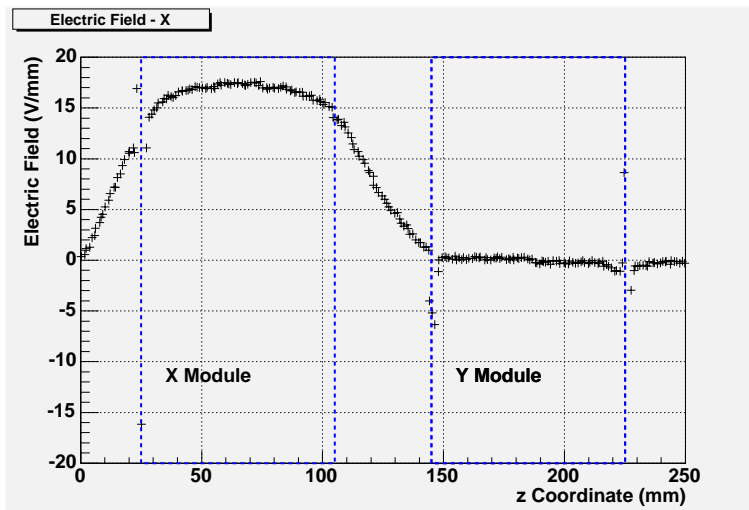


Figure 8: X component of beam-axis electric field across entire TEC. The positions of the X and Y modules are indicated

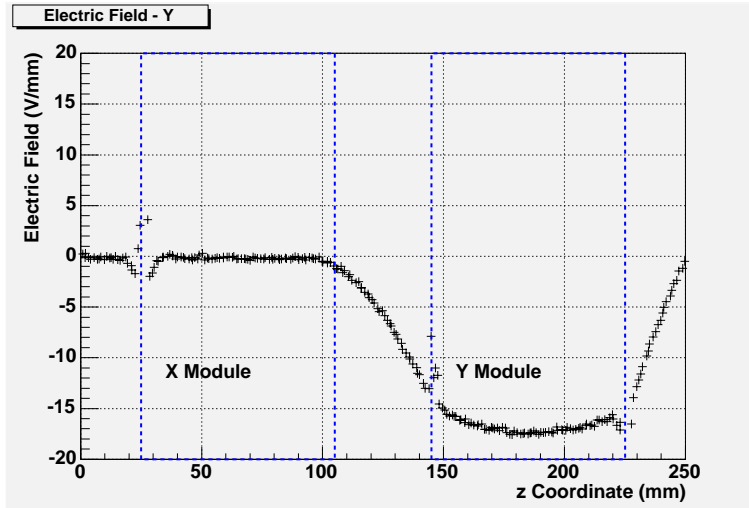


Figure 9: Y component of beam-axis electric field across entire TEC.

1. Wall Effects
2. Poor Drift Volume Separation
3. Edge Effects
4. Module Interference

### 2.2.1 Wall Effects

The grounded gas chamber walls have a minor effect on the electric field. Figure 10 shows the shape of the field at the center of one module across the wire-plane. This module is placed in the middle of a grounded gas box to study the effects of the walls on the field. Distance from the module to the box wall is the same as in the real TEC geometry.

The difference between the “wall effect” part of the plot and the “nominal” plot is a result of an increase in distance to the ground gas-box walls by a factor of 5. Examining the dominant field component, Y, a maximum difference of

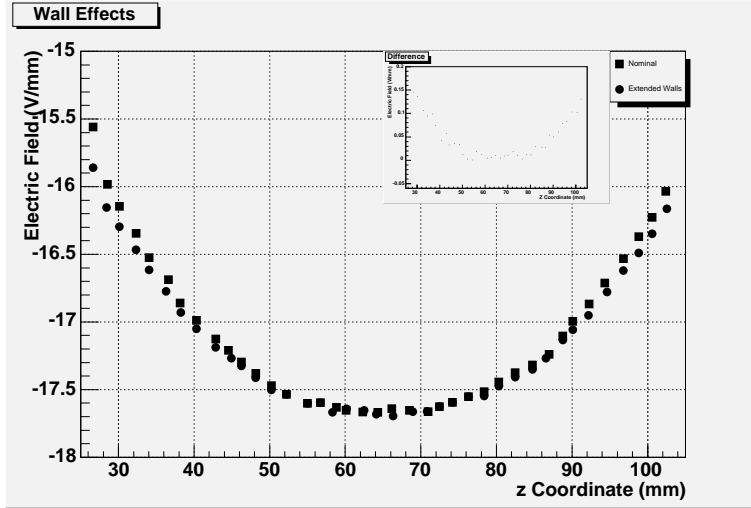


Figure 10: Dominant field in a single module. Gas box walls are extended by a factor of 5 to display effect of gas box wall.

about 0.15 V/mm (1% of the ideal field) exists near the edges of the wire-plane. This effect would only exist in the real geometry on one side of each module.

The effects of the walls could potentially be alleviated by modifications to the field cage to better shape the potential near the walls. One such modification discussed later is the replacement of the wire-planes with aluminized mylar strips.

### 2.2.2 Drift Volume Separation

Ideally the two drift volumes of the TEC are separated by the grounded grid plane and their fields are constant. In reality, the figure 8 indicates the drift volume field varies by up to 2.4 V/mm (15% of ideal field) over the length of the module. A clear curve is visible. Examining the module's dominant field more closely yields figure 11, which is the dominant field in the y-module across the wire-planes in the center of the module. Also shown on figure 11 is the field when the sense plane is turned off. There is a reduction in the field intensity –

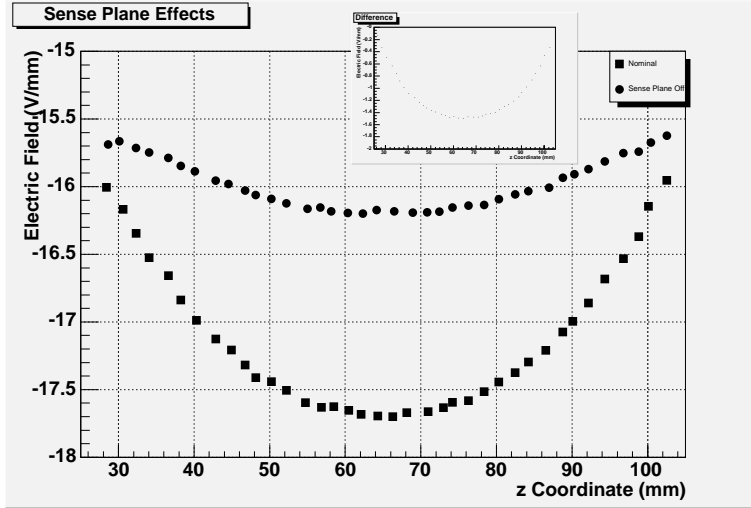


Figure 11: Dominant field in a single module. Sense plane on and off are shown to study its effects on the dominant field.

up to about 1V/mm (6% of the ideal field). The grid plane, in the simulation, is not effective in separating the drift volumes.

Figure 7 shows the shape of the field on axis for the y-module for various resolution meshings of the sense/grid planes. Also shown is the solution for physical wire strips (forced meshing). It is clear while the sense plane effect on the drift volume field is reduced when resolution is increased, the shape remains the same, and the effect magnitude approaches that of the physical wires. This shows that the effect is not an artifact of the plane potential meshing method. The z asymmetries in these plots appear due to low resolution in field cage planes similar to figure 6, showing low resolution field cage effects.

### 2.2.3 Edge Effects

The shape of the field in the drift region is not completely the result of the sense plane. When turned off, seen in figure 11 the field is still curved - varying by up to 0.5 V/mm (3% of the ideal field) over the module. This could possibly be

due to a feature of the geometry, a resolution problem, or both.

Figure 2 shows the a slice of a TEC module. Modeled after parallel potential planes, the ideal potential in the drift volume is set by the -1kV potential plane (bottom) and the grounded grid plane. A possible source of the edge effects is the field influence of the upper ground plate.

Another possibility is the failure of the simulation to represent the field cage wires. Figure 6 shows the effects of increasing resolution in the field cage wires. Similar to the sense plane wire effects, the effects are similar in shape, but reduce in magnitude.

#### 2.2.4 Module Interference

A final source of field irregularity could come from interference between the two modules. To analyze the field of the x module was analyzed, in the zx plane down the center ( $y=0$ ), for the nominal configuration, as well as when the opposite module (y module) was turned off. Figures 12-14 are the difference plots for each component of the field. They are shown over the x module, so the dominant field is in the x direction.

Figure 12 shows an interference on the order of 1% of the mean field through the module. Shown is the interference in XZ. The Y module center is at  $z=185\text{mm}$ . Toward the sense plane ( upper region of figure 12 ) the interference is negative, indicating an increase in field strength when the y module is on (dominant field points in the negative direction). In the lower region, the field interference is positive resulting in a reduction of the dominant field.

Figure 13 shows a leaking of the Y component of the field from the Y module into the X module. The magnitude of this interference is about half that of the interference in the X direction.

The interference is most seen in the Z component of the field (toward the Y module) shown in figure 14.

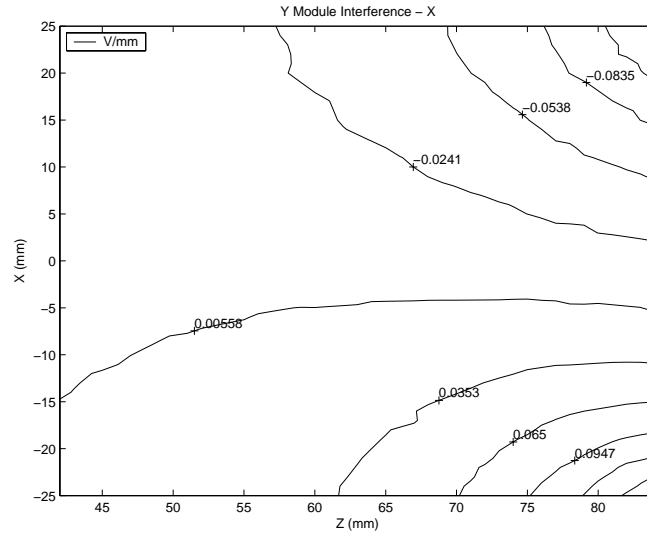


Figure 12: Module interference over X module - X field component

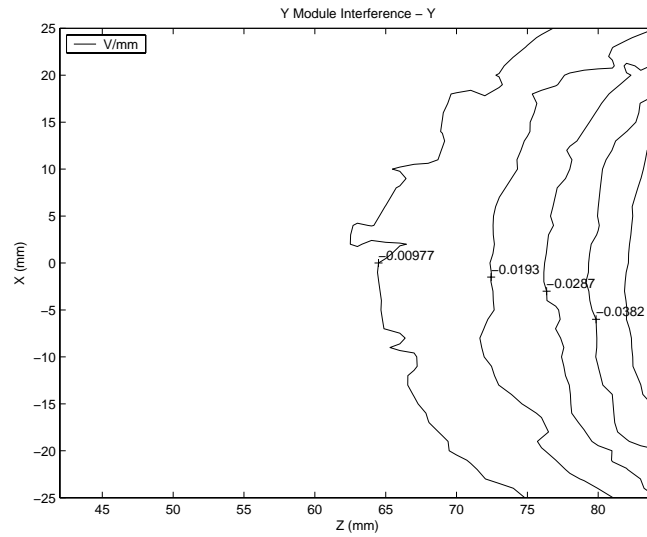


Figure 13: Module interference over X module - Y field component

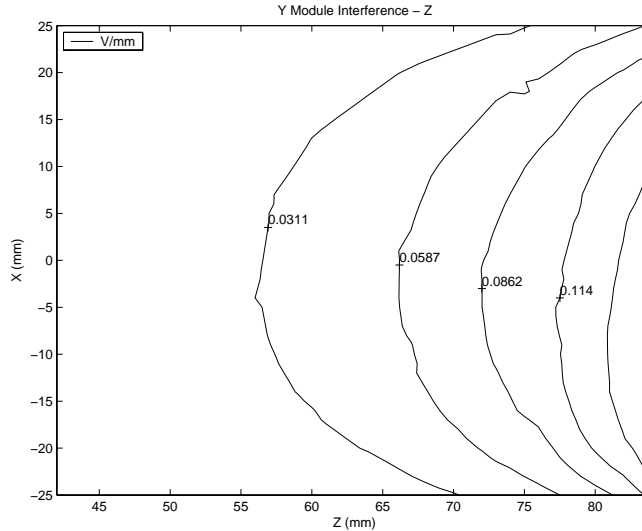


Figure 14: Module interference over X module - Z field component

## 2.3 TEC Modifications

### 2.3.1 Grid Plane Extension

One possible way to force the shape of the field in the drift region into a more constant shape is to modify the ground plane. Figure 11 shows the shape of the field when the sense plane is turned off. Without the sense plane effect, there is still a curvature, that can not be completely attributed to the failure of the field cage wires.

To further shield the drift region from the effects of the sense plane and upper ground plane, the grid plane can be extended to the out to the field cage wires. A grounded layer of conducting material attached to the grid plane extending to the field-cage would accomplish this, shown in blue in figure 15

Figure 16 shows the effects of this extension. The plot appears asymmetrical in z because of a poor meshing quality in the field cage. From a first look, the extension appears to decrease the field in the y direction. Shown also is the difference plot (extension off - extension on). In magnitude, the grid plane

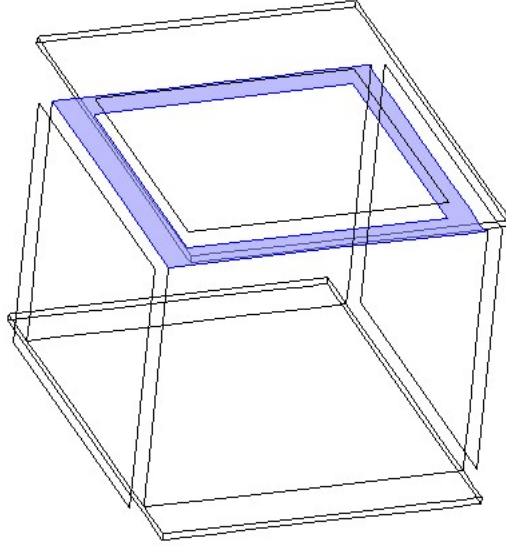


Figure 15: The geometry of the grid plane extension is shown in blue. It consists of extending the grounded region on the grid plane beyond the wires, adding conducting grounded material to the existing structure.

extension has the effect of decreasing the field by about 0.6% directly under the extension ( $z = 32-42$  and  $z = 88-98$ ). Examining figure 11, the field variations in this region require up to a 6% decrease in field. The grid plane extension aids in smoothing the field, but is not sufficient to overcome the full edge effects.

### 2.3.2 Module Separators

Wire-plane module separators were proposed to eliminate the interference between the modules. The idea is to “block” the interference by setting the potential between the modules where it is not well defined. When considering such a modification, both the effectiveness of eliminating the interference, as well as the effect on the field shape should be considered.

Two geometries were considered. The first involves separating the modules by a single wire-plane of set potential. The addition of the grounded wire-plane between the produces a similar effect on the Y field as the wall effects discussed

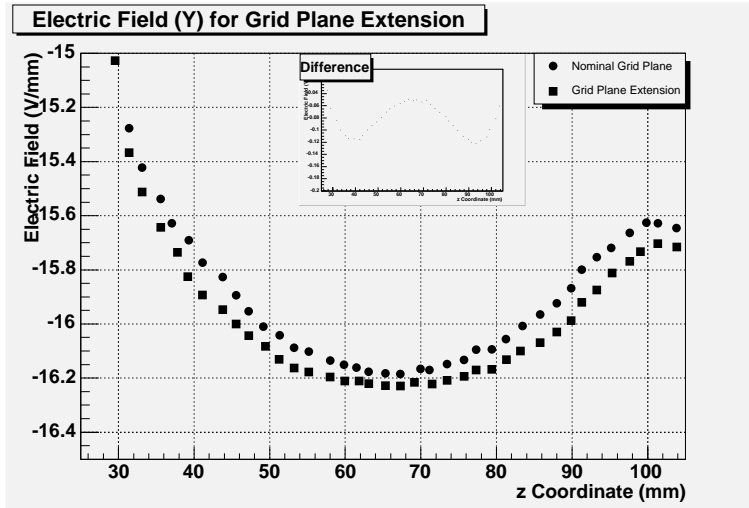


Figure 16: Effect of grid plane extension. A plot of the Y field in the y module with the sense plane turned off. Plot appears asymmetrical in z due to low field cage resolution. Plotted are the nominal geometry and grid plane extension fields down the module center. Shown also is the difference plot (extension off - extension on).

above. Figure 17 shows the field cage extension approach. Shown in blue, planes identical to the field cages of each module are placed 15mm from the field cages, in the center of the gas box. The desired effect is extending the field of each module, allowing for a well defined, constant field in the interior.

Figures 18-20 show the resulting interference when the field cage separators are used. The interference is reduced by a factor of roughly 2.5 when compared to the nominal geometry in figures 12-14.

### 2.3.3 Mylar Field-cage

A proposed modification to the field-cage involves replacing the wires and strips with an aluminized mylar foil. This foil would have the same potential as the wires and strips and contain 23 aluminized sections.

Figure 21 shows the shape of the field with the aluminized mylar field-cage.

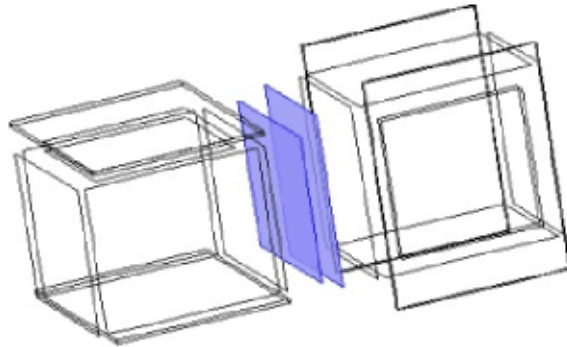


Figure 17: The geometry of the field cage extension separators. They are simulated as exact copies of the field cage wire-planes from each module.

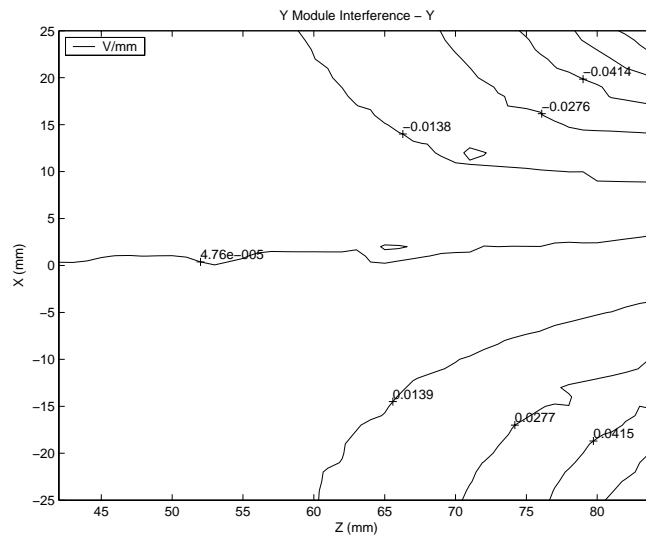


Figure 18: Module interference with added field cage extension - X component

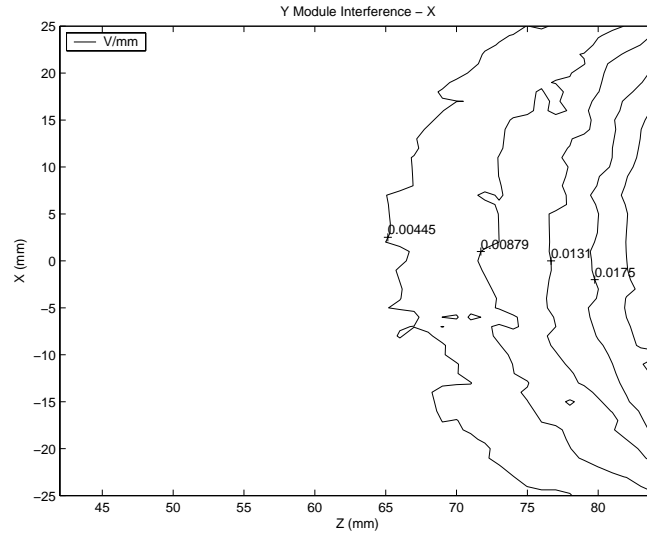


Figure 19: Module interference with added field cage extension - Y component

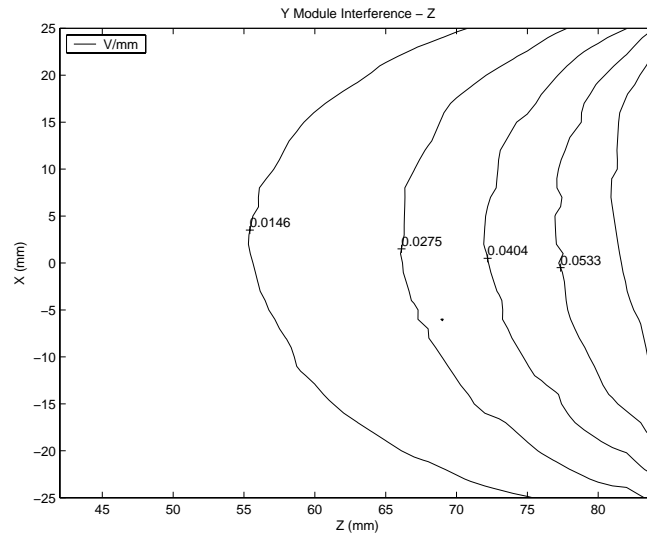


Figure 20: Module interference with added field cage extension - Z component

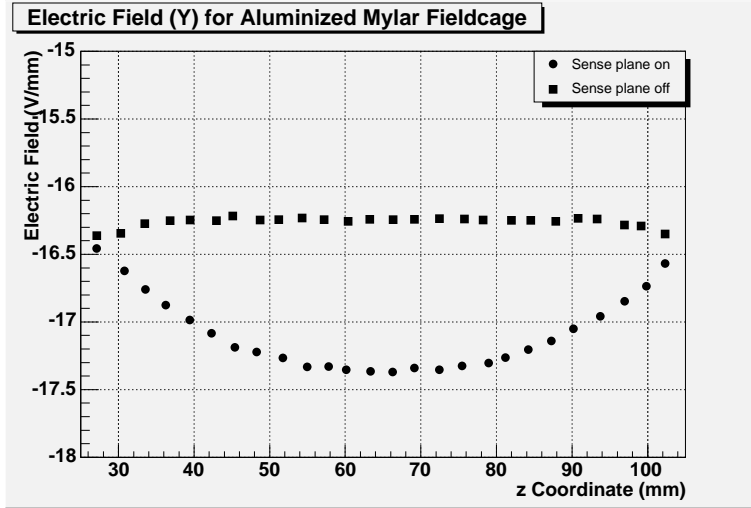


Figure 21: Field shape down beam axis with aluminized mylar field cage

Clearly the edge effects are reduced significantly. With the sense plane off, the aluminized mylar is able to produce a nearly constant field across the module. It appears the mylar field-cage is able to negate the edge effects with much more success than the standard field-cage and the grid plane extension.

### 3 Conclusions

The simulation detailed in this report is a reasonable approximation to reality. The geometry used was placed according to schematics in the millimeter precision. Effects of wire plane approximations on results have been explored. Results produced are useful in a qualitative study of the electric field of the TEC modules.

A first solution to for the electric field indicated a variation in dominant field in both modules of up to 2.4 V/mm (15% of the ideal field). The field inside each module had a curved shape, consistent with failure in the field cage to negate the edge effects of the design. The grounded gas box walls at a distance

of 25.4mm from the module field-cage were found to decrease the field by up to 0.15 (1% ideal field) over the module. The grid plane was found to be unable to completely separate the drift regions resulting in the high voltage sense plane altering the field by up to 1V/mm (6% ideal field) in the center of the module. The edge effects were attributed to up to 0.5V/mm (3% of ideal field) variation in field magnitude.

Effects of geometry alterations were studied. The grid plane extension was found to provide about a 0.15 V/mm (1%) improvement in edge effects. The field cage extension module separators provided a reduction in module interference of about a factor of 2.5 and had a minimal effect on the module field shape. The mylar field-cage alterations produced the most constant module electric field than any other alteration.